Mode specific excited state dynamics study of bis(phenylethynyl)benzene from ultrafast Raman loss spectroscopy

Khokan Roy, Surajit Kayal, Freek Ariese, Andrew Beeby, and Siva Umapathy

Citation: The Journal of Chemical Physics **146**, 064303 (2017); doi: 10.1063/1.4975174
View online: http://dx.doi.org/10.1063/1.4975174
View Table of Contents: http://aip.scitation.org/toc/jcp/146/6
Published by the American Institute of Physics

Mode specific excited state dynamics study of bis(phenylethynyl)benzene from ultrafast Raman loss spectroscopy

Khokan Roy,[1] Surajit Kayal,[1] Freek Ariese,[2] Andrew Beeby,[3] and Siva Umapathy[1,4,a)]
[1]*Department of Inorganic and Physical Chemistry, Indian Institute of Science, Bangalore 560012, India*
[2]*On leave from LaserLaB, VU University Amsterdam, De Boelelaan 1081, 1081 HV Amsterdam, Netherlands*
[3]*Department of Chemistry, University of Durham, South Road, Durham DH1 3LE, United Kingdom*
[4]*Department of Instrumentation and Applied Physics, Indian Institute of Science, Bangalore 560012, India*

(Received 18 October 2016; accepted 18 January 2017; published online 8 February 2017)

Femtosecond transient absorption (fs-TA) and Ultrafast Raman Loss Spectroscopy (URLS) have been applied to reveal the excited state dynamics of bis(phenylethynyl)benzene (BPEB), a model system for one-dimensional molecular wires that have numerous applications in opto-electronics. It is known from the literature that in the ground state BPEB has a low torsional barrier, resulting in a mixed population of rotamers in solution at room temperature. For the excited state this torsional barrier had been calculated to be much higher. Our femtosecond TA measurements show a multi-exponential behaviour, related to the complex structural dynamics in the excited electronic state. Time-resolved, excited state URLS studies in different solvents reveal mode-dependent kinetics and picosecond vibrational relaxation dynamics of high frequency vibrations. After excitation, a gradual increase in intensity is observed for all Raman bands, which reflects the structural reorganization of Franck-Condon excited, non-planar rotamers to a planar conformation. It is argued that this excited state planarization is also responsible for its high fluorescence quantum yield. The time dependent peak positions of high frequency vibrations provide additional information: a rapid, sub-picosecond decrease in peak frequency, followed by a slower increase, indicates the extent of conjugation during different phases of excited state relaxation. The CC triple (—C≡C—) bond responds somewhat faster to structural reorganization than the CC double (>C═C<) bonds. This study deepens our understanding of the excited state of BPEB and analogous linear pi-conjugated systems and may thus contribute to the advancement of polymeric "molecular wires." *Published by AIP Publishing.* [http://dx.doi.org/10.1063/1.4975174]

I. INTRODUCTION

Linear pi-conjugated systems, which are well known as "molecular wires" are an important class of materials having numerous applications in the opto-electronics field.[1,2] Typically, systems possessing close-coupled (CC) triple (—C≡C—) bonds in conjugation with planar, aromatic chromophores fall into this category (Fig. 1). The two orthogonal π-bonds between two carbon atoms make the electron cloud around the CC triple bond cylindrical in nature. Furthermore, chromophores connected through single bonds with the CC triple bond enjoy some degree of conjugation at diverse dihedral angles of the chromophores, which is very different from the CC double (>C═C<) bond conjugated systems, where there is no overlap of the π-orbitals at 90°. So, CC triple bonded systems are linear and maintain some degree of electron delocalization throughout the entire molecular backbone. A deeper understanding of the photophysics, the energy transfer from the excited state, and the vibrational dynamics of such systems will be useful for designing opto-electronic devices.[3] Excited state dynamics of π-conjugated small organic molecules has been studied by many groups using time resolved vibrational spectroscopic techniques (both in the time and frequency domains) to understand structural dynamics.[4–18] Interestingly, Chen *et al.* reported that for such systems the switching between conducting and non-conducting states appears to be related to the dihedral angles between the chromophores.[19,20]

The photophysical properties of 1,4-bis(phenylethynyl) benzene (BPEB) (Fig. 1), which is generally regarded as the smallest unit that resembles polymeric phenylethynylenes, have been well studied at room temperature as well as at low temperatures.[21–23] Partially structured absorption and emission spectra were observed at room temperature in solutions and this has been attributed to S_0-S_1 transitions of the same molecule with different structural conformations.[21,24] In the ground state, the rotational barrier around the sp^2-sp CC single bond is very low; it was determined by Greaves *et al.* to be 220-235 cm^{-1} from a jet spectroscopy experiment, and this number agrees with the AM1 calculations of Levitus (0.5 kcal/mol = 180 cm^{-1}).[25,26] Therefore, all rotamers ranging from planar to twisted forms are likely to co-exist at room temperature, resulting in electronic transitions at different energies. However, in the excited state, the energy difference between the planar and the twisted conformation is believed to be much larger: 15 kcal/mol.[27] Interestingly, low-temperature absorption and fluorescence studies show more

a)Author to whom correspondence should be addressed. Electronic mail: umapathy@ipc.iisc.ernet.in

FIG. 1. Molecular structure of BPEB in planar conformation.

structured vibronic bands, attributed to the progression of high-frequency vibrations of BPEB. Furthermore, it is reported that the mirror image symmetry of the low-temperature absorption and emission spectra confirms the similarity of the absorbing and emitting geometries.[21,23] This suggests that, although at room temperature there are multiple conformers in the ground state, on excitation the excited state geometry seems to relax to a single conformer. However, there is some disagreement regarding the geometry and extent of electronic delocalization of the excited state of BPEB. For example, cumulenic and quinoidal geometries were proposed by Sluch *et al.*,[28] but a time-resolved picosecond study by Beeby *et al.* has ruled out the presence of such structures for the excited electronic state. Those time resolved fluorescence studies showed a slow (tens of picoseconds) rising component that has been attributed to structural reorganization in the excited electronic state.[24]

Thus, in order to better understand the structural dynamics of the photophysical states, we have explored the excited electronic state dynamics of BPEB using femtosecond transient absorption (TA) and the vibrational mode-dependent dynamics using ultrafast Raman loss spectroscopy (URLS). URLS is analogous to femtosecond stimulated Raman spectroscopy (FSRS) but the Raman spectra are measured in the anti-Stokes region with high signal-to-noise ratios.[29–39] Based on the literature, it was expected that in the excited state major conformational changes could occur. The objective of this work is to study the vibrational mode-specific dynamics at femtosecond time scales within the context of structural reorganization and understand the contribution of different modes towards excited state planarization and their instantaneous frequency response. Finally, we aim to increase our understanding of the role of solvent properties in the excited-state mode-dependent dynamics.

II. EXPERIMENTAL METHODS

A. Sample preparation and steady state measurements

1,4-bis(phenylethynyl)benzene was prepared by the Sonogashira coupling of 1,4-di-iodobenzene and phenylacetylene.[1] The physical state of the compound at room temperature is solid powder. The purity of the sample was checked using UV-Visible (UV-Vis) absorption and fluorescence spectroscopy (see Sec. III A). The solvents methanol (MeOH), acetonitrile (ACN), and butyronitrile (BuCN) used for the experiments were HPLC grade and were purchased from Sigma-Aldrich. Ground state absorption measurements were carried out using a Perkin Elmer UV WinLab Lambda 900 UV-Vis spectrometer. Fluorescence measurements were carried out with a Fluoromax 4 spectrofluorometer. For excitation wavelength dependent fluorescence, all other parameters such as slit width and concentration were kept constant. All measurements were carried out at room temperature.

B. Transient absorption and URLS setup

The femtosecond Transient Absorption (fs-TA) and URLS setup (see Fig. 2) is based on a Spectra Physics Spitfire Pro Ti:sapphire oscillator-regenerative amplifier system. The amplifier delivers pulses of 790 nm wavelength with 100 fs duration at a repetition rate of 1 kHz and 2 mJ energy per pulse. Half of the amplifier output (1 mJ) was used as input for the OPA (Optical Parametric Amplifier). The other half was used as input for TOPAS-Light Conversion (Travelling Wave Optical Parametric Amplifier of Super-fluorescence) to yield 5–10 μJ/pulse at 307 nm. Using a neutral density filter, the power was adjusted to 1 μJ at the sample. The tunability range of the OPA is 480–800 nm; this output was used to generate the Raman pump (RP) pulse in the visible region. The narrow-band Raman pump (ps pulses) was generated using a 4f-grating pair configuration.[24] This study was performed with 300 nJ Raman pump pulses having 15–18 cm^{-1} spectral width

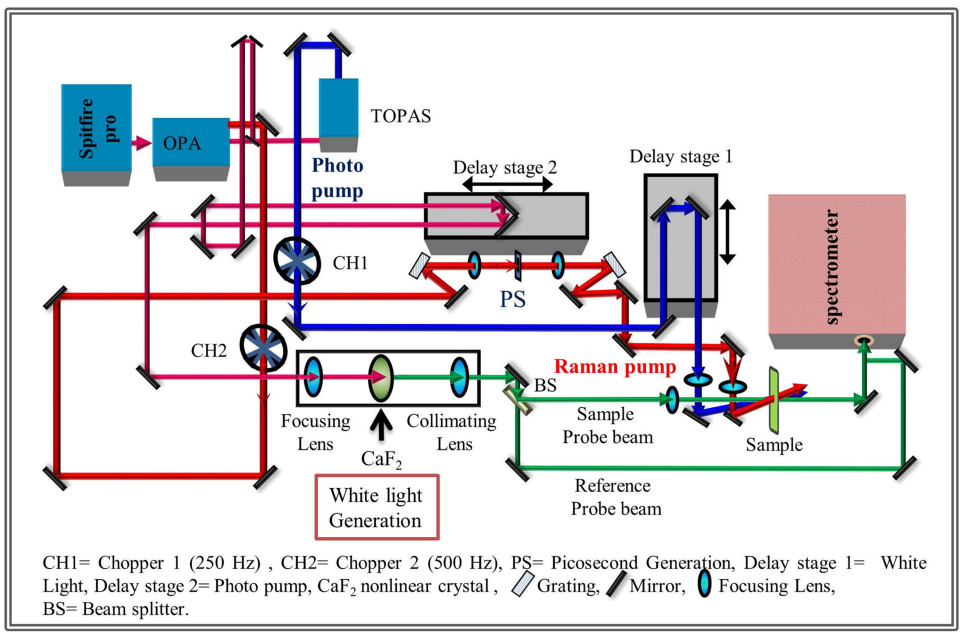

FIG. 2. Experimental setup for URLS and fs-TA; for femtosecond transient absorption only the actinic pump and white light probe are used.

(FWHM). For the current URLS measurements, the Raman pump was tuned to 622 nm which is the peak wavelength obtained from transient absorption measurements with 307 nm photo pump (PP) excitation. The Raman probe pulse was generated from the remainder of the amplifier output (40 μJ); the Spitfire output fundamental beam was focused in a 3 mm thick sapphire crystal which generates a broadband super continuum white light (WL). The WL probe beam was sent to the sample after a 50:50 beam-splitter (30:30 nJ). The probe beam was spatially and temporally overlapped with the photo pump and the Raman pump beams at the cuvette. The other half of the probe beam was passed through a different path for reference correction. All URLS measurements were performed in a 1 mm flow type cuvette, where the sample solution was circulated to avoid exposure of the sample to multiple shots of the laser. The transmitted probe beam was directed to the entrance plane of a 550 Triax spectrograph, equipped with a dual array detector for both sample and reference probe spectra. It has been designed to facilitate the readout of individual laser pulses at 1 kHz. In the experimental setup shown in Fig. 2, the WL beams (probe and reference) are aligned on top of each other, separated vertically by 12 mm with respect to the optical axis of the spectrometer. The other beams (Raman pump and photo pump) are combined spatially with the WL at the sample point in a non-collinear manner, which ensures that the Raman pump and photo pump are not entering the spectrograph. The photo pump is focused using a 150-mm focal length lens much before the sample point to ensure a larger waist size at the sample point as compared to the Raman pump and WL. The actinic photo pump, followed after a delay by the interaction of the WL beam and the Raman pump with the sample, leads to the generation of the excited state URLS signal riding on the WL background, which is recorded by the spectrograph and detector. Further technical details of the instrument will be published elsewhere.

Transient measurements were carried out in shot-to-shot detection fashion. For URLS, a four-cycle pulse sequence is controlled by two mechanical choppers positioned in the Raman pump (RP) and photo pump (PP) beam paths. Chopper CH1 in the PP path runs at 250 Hz and chopper CH2 in the RP path runs at 500 Hz frequency. The WL beam, which is used for transient absorption and as transient URLS probe, runs at 1 kHz repetition rate and one filter wheel is kept in that beam path for background correction before each measurement. It blocks the WL before every scan and subtracts the background from the signal. For TA measurements, chopper CH1 in the PP path runs at 500 Hz and the data acquisition system works at a two pulse cycle (probe only and probe + PP) to make the measurement faster as compared to the four-pulse cycle (used for transient URLS). The pump probe geometry for fs-TA measurements was kept at magic angle (54.7°) to eliminate the contribution from rotational diffusion of solute molecules on the transient decay signal.[40–43] However, in the case of transient URLS measurements, experiments were performed in parallel configuration in order to obtain a better signal-to-noise ratio. The time resolution for both fs-TA and URLS is ~200 fs. In the case of TA, excitation was chosen in such a way as to get a maximum population in the excited electronic state. The 307-nm photo pump is close to the ground state absorption maximum. The optical density of BPEB in methanol at this wavelength was around 1 in a 1-mm pathlength cuvette. To avoid multiple shot exposures from the excitation pump, the experiment was carried out in a flow type cuvette and the sample solution flowed at a rate sufficient to avoid overlap of the excited volume with the next laser pulse. Spectra were recorded over the −20 to 1500 ps time window, divided into several sub-windows to capture the multi-exponential dynamics of the species under investigation. The smallest steps (10 fs) were taken from −0.3 to 2 ps. This range contained time zero, exponential rise, and starting of the exponential decay of all the Raman bands. All transient URLS data were analysed after time zero and chirp correction.

Collected data are extracted from the data acquisition system for further processing. The URLS spectra have an inherent background apart from the transient absorption background, so background subtraction is necessary. The background was subtracted using a higher order polynomial. The baseline corrected and background subtracted data were fitted using Origin 8.5 and Matlab for several time points. The built-in Gaussian amplitude function was used to fit the URLS peaks over the whole spectral window. An iterative least-square method was implemented to optimize the fitting parameters. The goodness of fit was ensured by reducing chi-square values and optimizing R (least square) values.

III. RESULTS

A. UV-Vis and fluorescence studies

The absorption spectrum of BPEB is not very sensitive to the solvent. Absorption spectra obtained in different solvents of increasing polarity show only a minor blue shift of approximately 100 cm^{-1} (not shown). This indicates that the dipole moment of the molecule in the ground and excited states is not very different. The absorption spectrum has some vibronic structure which may be due to vibrational progression of highly Franck-Condon active modes having a significant amount of distortion in the excited electronic state.[23] Alternatively, these partially structured absorption spectra may also be due to the transitions to higher electronic states, but according to James *et al.* those states do not have a significant oscillator strength.[27] It has been reported by Levitus *et al.* that in the ground state BPEB can exist as a mixture of rotamers because of the low rotational barrier of 0.5 kcal/mol (180 cm^{-1}) which is below kT.[18,19] The low temperature absorption studies by Chu and Pang showed that at −198 °C (75.15 K) the absorption spectrum becomes sharper and the relative intensity of the 0-0 band increases.[16] A relatively strong 0-0 band has also been observed in the fluorescence spectrum of BPEB in methanol shown in Fig. 3(a). The region shared by both absorption and fluorescence bands indicates the 0-0 transition for the system. The spectra are not an exact mirror image of each other at room temperature but at low temperature they show better mirror image symmetry.[23] This could indicate that at low temperature, the dominant absorbing species is similar to the emitting species, whereas at room temperature other conformers also contribute to the absorption spectrum. The fluorescence spectra do not show significant differences in spectral shape for

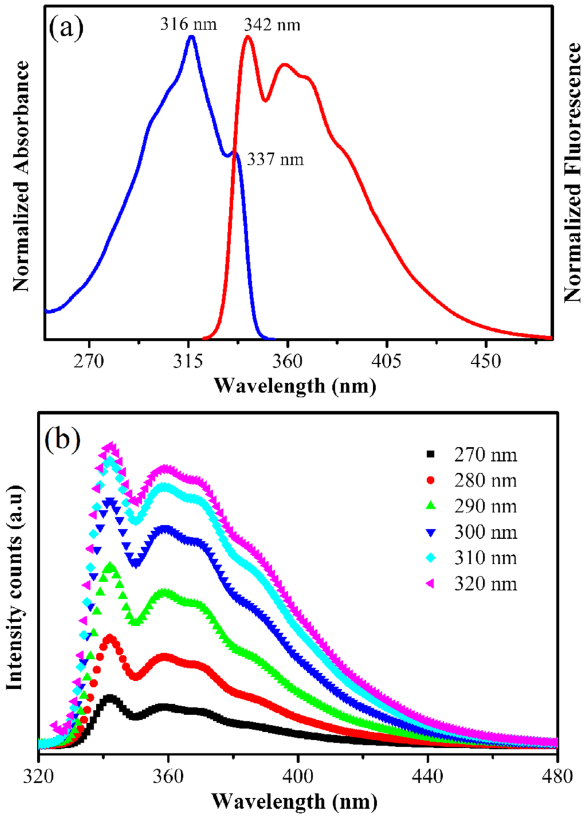

FIG. 3. (a) Ground state absorption and emission spectra of BPEB in methanol, shown on the same scale for ease of comparison. (b) Excitation wavelength dependent emission spectra show no sign of multiple emitting species.

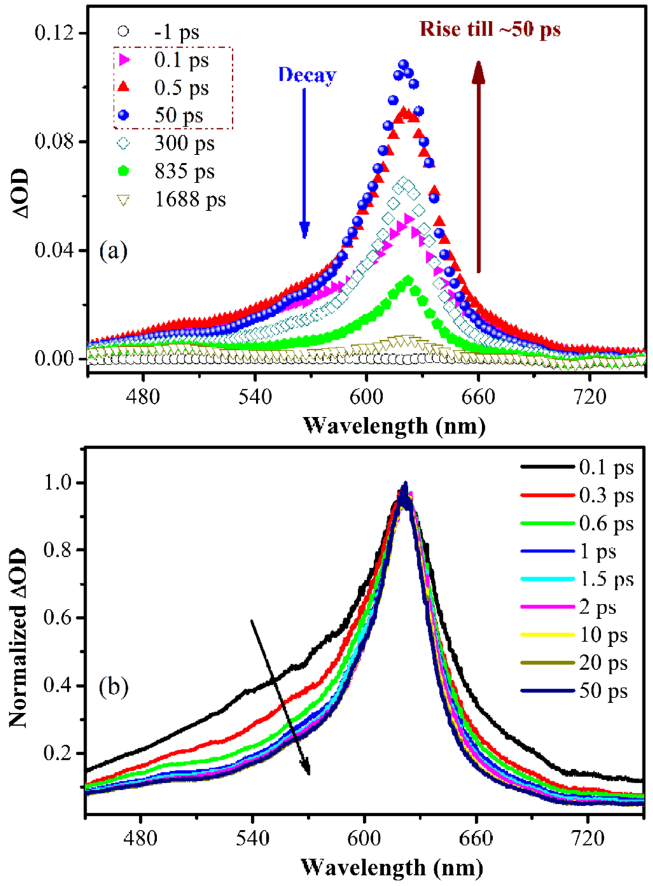

FIG. 4. (a) TA spectra of BPEB at different time delays in methanol solvent. (b) Normalized TA spectra for different time delays, showing spectral changes at ultrafast time scales.

various excitation wavelengths (see Fig. 3(b)), which indicates that the emission is probably due to a single emitting species.[27] The two distinct emission spectra and extra absorption band at 365 nm reported by Levitus *et al.* were not observed in our experiments, indicating a higher purity of the sample.[26]

B. Femtosecond transient absorption measurements

We have employed fs-TA spectroscopy to study the excited state dynamics of BPEB in methanol, acetonitrile, and butyronitrile solvents at a concentration of 200 μmol. In this experiment, a femtosecond pump pulse at 307 nm generated the transient species in the first excited singlet state. The TA spectra were measured under magic angle conditions by a delayed femtosecond probe pulse provided by the WL continuum. The changes in the transient species absorbance were measured for the whole wavelength range (430–750 nm) simultaneously, at time delays ranging from −20 to 1800 ps. Selected transient absorption spectra of BPEB in methanol at different delay times are shown in Fig. 4, before and after normalization. The excited state absorption maximum at 621 nm and a shoulder around 560 nm were observed for all the time delays; the latter could be assigned as a vibronic progression of a high frequency vibration of the excited singlet state. The excited state maximum does not shift much during the time evolution, but the broad blue-shifted band at about 540 nm is observed only at sub-ps time scales. At longer delays this band disappears and the 621 nm peak becomes sharper. A major change was observed in the intensity, which showed a multiphasic behaviour with time. Most of the prominent changes were observed within the 100 ps time scale. The multi-exponential behaviour of chirp corrected data was analysed globally with an exponential decay function of the form,

$$A(t) = [A_1 * e^{-\frac{t}{\tau 1}} + A_2 * e^{-\frac{t}{\tau 2}} + A_3 * e^{-\frac{t}{\tau 3}}], \quad (1)$$

where A_i denotes the amplitude (related to the concentration of the species involved in the photophysical processes) and τ_i denotes the lifetime of that individual species. The multi-exponential kinetics was deconvoluted with the instrument response function (IRF). Rise and decay curves of BPEB following excitation at 307 nm are shown for the wavelength 621 nm in Fig. S1 (supplementary material). The resulting kinetic parameters obtained from multi-exponential fitting are shown in Table I.

TABLE I. Multi-exponential global fitting parameters of the transient absorption signal of BPEB in different solvents.

Solvents	τ_1(ps)[a]	τ_2(ps)[a]	τ_3(ps)[a]
MeOH	0.5	8	480
ACN	0.6	20	515
BuCN	1.3	20	535

[a]τ_1 and τ_2 correspond with rises and τ_3 describes the decay kinetics.

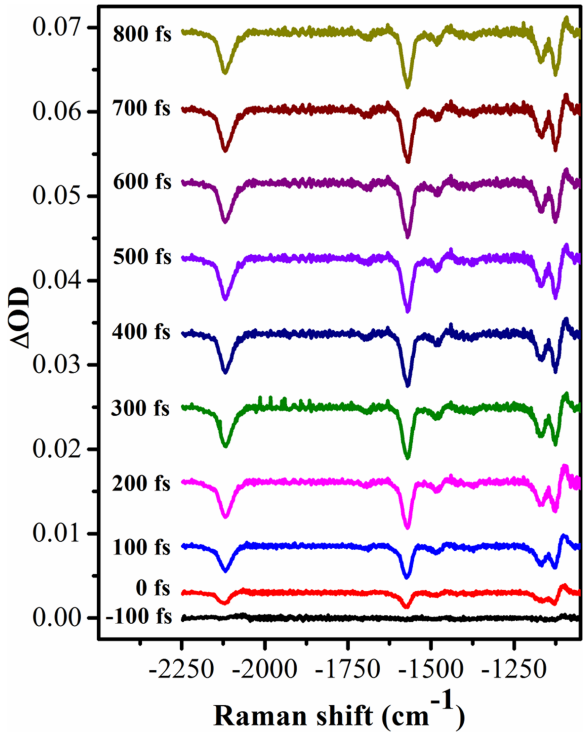

FIG. 5. Representative transient URLS spectra of the excited singlet state of BPEB at sub-picosecond time scales. Spectra are vertically offset for clarity.

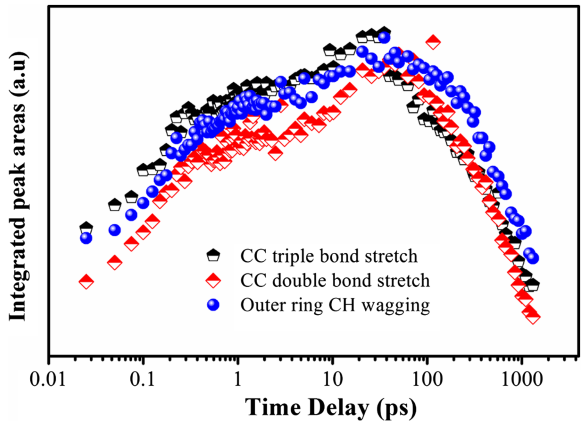

FIG. 6. Evolution of the integrated peak areas of the three major excited state Raman bands of BPEB in MeOH, shown on a logarithmic time scale. URLS peak areas are not to scale.

C. URLS measurements

The spectrally broad absorption, fluorescence, and femtosecond transient absorption spectra of BPEB did not yield much information about the vibrational dynamics during the structural reorganization.[24,25] In general, transient absorption provides information on the time dependent response due to the population dynamics and/or conformational changes in the excited electronic states. However, any involvement of the Franck-Condon active vibrational modes remains invisible under the broad excited state absorption bands, which makes it difficult to elucidate the structural vibrations involved during the time dependent nuclear dynamics. Representative URLS spectra of excited state of BPEB in methanol at delays from −100 fs to 800 fs are shown in Fig. 5; URLS spectra at other delay times are given in the supplementary material, Fig. S2. All measurements were carried out in the 1000–2200 cm^{-1} spectral window to monitor the changes in the high frequency modes. The strongest vibrational modes observed in this experiment were at 2126, 1573, 1173, and 1130 cm^{-1}, which agree well with the excited state resonance Raman spectrum reported by Beeby *et al.*[24] These bands have been assigned to localized vibrational motion of the ethyne groups (2126 cm^{-1}), symmetric stretch of all three aromatic rings along the molecular long axis (1573 cm^{-1}), and the region 1130–1170 cm^{-1} corresponds to symmetric bending modes. The latter are clearly resolved in the URLS data, having contributions from both the inner and the outer rings' bending vibrations.[24] The dispersive line shape observed for the bending vibrations is probably related to the resonance effects described by Frontiera *et al.* and Umapathy *et al.*,[32] but it is less prominent for the higher-energy modes of the CC triple and CC double bonds. The excited state URLS bands fit well with the vibronic energy differences obtained from the low temperature absorption spectrum of BPEB at −198 °C published by Chu and Pang,[23] and also reasonably well with the broadened room temperature absorption of Fig. 3(a). In comparison with that of the ground state spontaneous Raman data, the carbon-carbon triple and aromatic double bonds in the URLS spectra show a significant redshift of almost 116 cm^{-1} and 31 cm^{-1}, respectively. This downshift of the Raman bands in the excited state points at a weakening of the bond strengths, as expected due to the π-π* transition. For the C—H scissoring and wagging vibrations, relatively minor red-shifts were observed of about of 5–6 cm^{-1} compared to the ground state. After curve fitting of the individual Raman bands at each time point, the kinetics of the integrated band areas of the aromatic CC double and CC triple bond stretching peaks are shown in Fig. 6. Tri-exponential fitting was performed using the same methodology as in the case of TA. The individual Raman band intensities show two phases of exponential rise, followed by a single-exponential decay. The instrumental response was taken into account during fitting. The triple exponential kinetics of the carbon-carbon triple bond reflect (Table II) 9.6% popula

TABLE II. Kinetic parameters obtained from tri-exponential single kinetic fitting of the integrated URLS peak areas of the CC triple and CC double bonds of BPEB in methanol.

	A_1[a]	$\tau_{1\,(rise)}$[b]	A_2[a]	$\tau_{2\,(rise)}$[b]	A_3[a]	$\tau_{3\,(decay)}$[b]
CC triple bond stretch	−9.6%	0.6 ps (±0.2)	−17%	8.0 ps (±2)	73%	500 ps (±60)
Aromatic CC double bond stretch	−6.5%	0.4 ps (±0.2)	−26%	18.0 ps (±4)	67.5%	515 ps (±50)

[a] A_i' is the amplitude of the species involved in the kinetics.
[b] τ_i' is the lifetime of the corresponding species associated with exponential rise or decay.

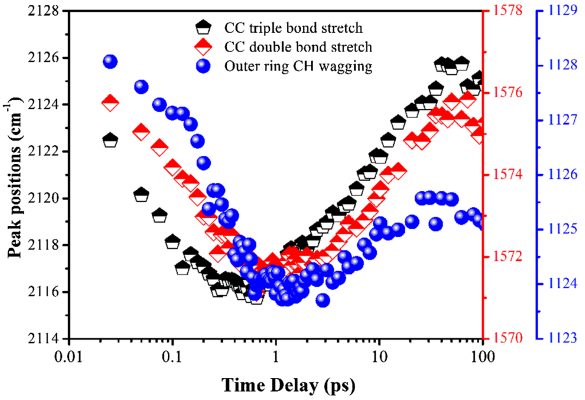

FIG. 7. Time dependent URLS peak positions of the three major excited state Raman bands of BPEB in MeOH, shown on a logarithmic time scale.

tion contribution with a 0.6 ps time constant (rise) and a 17% rising component with a 8 ps time constant, associated with the second phase of the intensity rise. The last component ~500 ps stands for the singlet state lifetime of the molecule with 73% contribution towards population decay.[24] The minor contribution from rotational diffusion, expected from a non-magic angle pump-probe configuration, did not appear in our fit, see Table II. The fitted curves on linear and logarithmic time scales are shown in Fig. S3 of the supplementary material.

The time dependent transient Raman band frequencies were further analyzed to obtain a deeper insight into the mode-dependent dynamics of excited BPEB. Individual bands were first fitted with a Gaussian amplitude function of the form $y = y_0 + A * e^{-\frac{(x-x_c)^2}{2w^2}}$, where A > 0, w > 0, y_0, x_c, w, and A are offset, centre, width, and amplitude, respectively, and $2w = \mathrm{FWHM}/\sqrt{\ln(4)}$. The fitting was carried out for several time points to get the maximum information on time dependent changes. Raw URLS spectra are shown in Fig. S5 and after smoothing in Fig. S6, for both triple bond and the double bond. The excited state URLS spectra yield the instantaneous frequencies of the evolving molecular structure on the excited potential energy surface. The time dependent frequencies (wavenumbers) of excited BPEB are shown in Fig. 7, with the time axis shown on a log scale to obtain a better visualization of the temporal evolution of the individual peaks. Up to 1 ps, all three major excited state Raman bands show a downshift of frequency with time. At a longer time scale the trend is opposite, and the peak frequencies increase up to 50–100 ps. The downshifts and upshifts are exponential in nature, which

TABLE III. Double exponential fitting parameters obtained from the time dependent URLS peak positions of the CC triple and CC double bond vibration obtained in different solvents.

Solvent	Band assignment	$\omega(\infty)^a$ cm^{-1}	$\delta\omega_1{}^b$ cm^{-1}	$\tau_1{}^c$ ps	$\delta\omega_2{}^b$ cm^{-1}	$\tau_2{}^c$ ps
Methanol	Localized C—C triple bond stretch	2126	6.7	0.1	−8.9	8.6
	Aromatic C=C stretch	1573	4.9	0.2	−4.0	12.1
Acetonitrile	Localized C—C triple bond stretch	2123	1.2	0.2	−8.6	12.0
	Aromatic C=C stretch	1579	2.8	0.4	−4.5	20.0
Butyronitrile	Localized C—C triple bond stretch	2118	3.7	0.1	−10.0	12.0
	Aromatic C=C stretch	1577	3.6	0.4	−5.0	19.0

[a] $\omega(\infty)$ corresponds with the vibrational frequency at semi-infinite time.
[b] $\delta\omega_1$ and $\delta\omega_2$ are the changes in vibrational frequency for the ultrafast downshift and the slower upshift.
[c] τ_1 and τ_2 are the time constants for the ultrafast downshift and the slower upshift of these vibrational frequencies.

is evident as shown in Figs. 8(a) and 8(b) for the CC triple and CC double bonds on a linear time scale. The time dependent peak positions of these modes show a similar behavior, but the extent of the down- and upshifts is different. These curves have been fitted with a double exponential function of the form

$$\omega(t) = \delta\omega 1 \exp\left(-\frac{t}{\tau_1}\right) + \delta\omega 2 \exp\left(-\frac{t}{\tau_2}\right) + \omega(\alpha), \quad (2)$$

where $\omega(\alpha)$ is the frequency of the fundamental at semi-infinite time, $\omega(t)$ the instantaneous frequency of the Raman band, $\delta\omega 1$ and $\delta\omega 2$ are the shifts in fundamental frequency due to structural changes in the excited state geometry, and τ_1 and τ_2 are the corresponding time constants. These time constants are listed in Table III and correspond to the initial sub-picosecond downshifts and slower (tens of picoseconds) upshifts of the observed high frequency Raman modes.

IV. DISCUSSION

A. Transient absorption global kinetics

The multi-exponential kinetics obtained from TA measurements of BPEB in methanol consist of an ultrafast component of around 0.5 ps (Table I) that contributes significantly

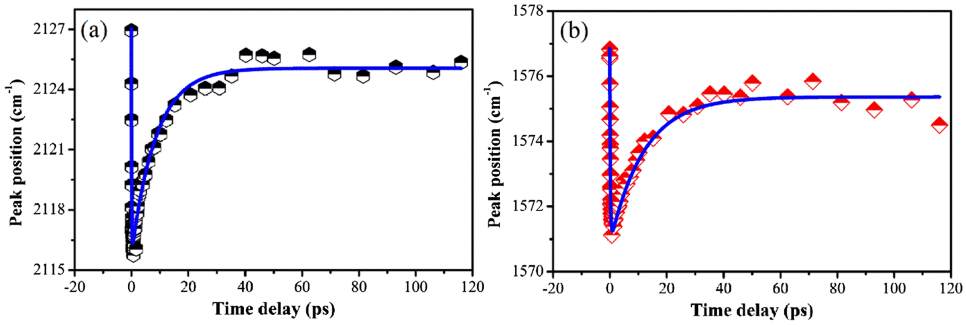

FIG. 8. Time dependent URLS peak positions of the CC triple (a) and CC double (b) bond vibrations of BPEB in MeOH, shown on a linear time scale.

to the intensity rise and can be assigned as planarization of twisted structures. Another component of about 8 ps also contributes to intensity growth, which could be due to the vibrational cooling of vibrationally hot molecules down the potential well of optically excited S_1 state. However, according to the time-resolved fluorescence study by Beeby *et al.*, a fluorescence intensity rise was observed over a few tens of picoseconds, with a change in the relative intensities of the vibronic structure.[24] This fact inspired us to assign the 8 ps component as structural reorganization which could be a second phase of planarization, although the molecular origin of this slower planarization process is still unknown to us. So, structural reorganization or slow planarization could be associated with vibrational cooling, which will be deciphered from the time dependent changes in vibrational frequency of the high frequency vibrations. Fig. S1 of the supplementary material shows an increase in the TA signal intensity up to a few tens of picoseconds. This fact is evident in Figs. 4(a) and 4(b) as well. There is an increase in TA intensity until 50 ps as shown by the upward arrow, followed by normal lifetime decay (downward arrow). The changes in spectral shape in Fig. 4(b) at ultrafast time scales clearly describe the first phase of planarization where the blue part of the spectrum (at 0.1 ps) rapidly merges into the spectrum of longer time scale. A thermally activated, highly twisted structure undergoes planarization with an ultrafast inertial response, which contributes to the increase in intensity. The third component, describing the decay phase, has a time constant of 480 ps, which is basically the lifetime of the excited state. The rate of the planarization is slightly lower in acetonitrile and butyronitrile, as shown in Table I. We hypothesize that, in methanol, the solvation shell would be hydrophobic in nature with the OH groups pointing away from BPEB as it is a non-polar molecule.[44] Such a solvation shell has less interaction with the solute inside it and the twisted structure can rotate faster as compared to acetonitrile and butyronitrile where such a hydrophobic solvation shell would not occur.[44] The equilibrium geometry after multiphase relaxation is planar and responsible for the efficient radiative emission from the singlet state. The longest lifetime of the S_1 state obtained from these femtosecond transient measurement is 480 ps in MeOH and somewhat longer in the two nitrile solvents, which is consistent with the fluorescence decay time of 530 ps reported by Beeby *et al.* for BPEB in cyclohexane.[24]

B. Mode dependent dynamics from the integrated URLS band areas

The kinetic analysis of the integrated areas of the URLS bands shows two exponential rise components with time (see Table II). The last component of ~500 ps is the lifetime of the S_1 state, which is similar as obtained from fs-TA. This multi-phasic behavior of intensity emerges clearly on a log scale, which is shown in Fig. 6. The initial rise is observed at a sub-picosecond time scale (0.4–0.6 ps) and a second phase of increase in intensity is observed up to a few tens of picoseconds (8–18 ps), followed by a single exponential decay. The first component was assigned as the first phase of planarization and the second rise component is related to the vibrational relaxation along with a second phase of planarization of the excited state species. All three major Raman bands show a similar trend during this time window. The increase in intensity is related to an increase in overall Raman cross section of the excited species. This dynamic polarization is related to the structural dynamics and time dependent geometry of the molecule. During the planarization phases, the transition dipole moment for $S_1 \rightarrow Sn$ transition becomes nuclear coordinate dependent (non-Condon effect), which leads to an increase in intensity in both fs-TA and URLS experiments. As compared to the 8 ps time constant determined for the CC triple bond, analysis of the CC double bond stretch yields a slightly longer time constant for the rise of ~18 ps, with a significant contribution towards the intensity rise (~26%). This slower rate is attributed to coupling of the acetylenic moiety with the phenyl rings. At the very beginning of planarization, the CC triple bonds' π-orbitals will optimize their interaction with the adjacent carbon atoms on the rings. This will be followed by nuclear motion of the rest of the phenyl groups, which have some degree of flexibility and of which large-scale displacements are hampered by solvent molecules. We propose that for this reason the CC triple bond intensity responds to planarization somewhat faster than that of the CC double bond. As discussed earlier, the non-planar conformer has a lower Raman polarizability and during the excited state time evolution it rearranges to a more stable planar state with a rise time of about 8–18 ps (see Table II and Fig. S3 of the supplementary material), which agrees with the rise time obtained from TA (see Table I). An overlay of the TA and URLS kinetics is given in the supplementary material (see Fig. S4) for better comparison. The similarity of the curves strongly suggests that the rising phases in the TA spectrum, presumably as a result of planarization and increase in conjugation, also result in a similar increase in URLS intensities because of the increase in polarizability. During this time, the phenyl rings rotate from some arbitrary Franck-Condon geometry to a planar conformer because in the excited state BPEB has a much higher rotational barrier along the sp^2-sp carbon—carbon single bonds as compared to the ground state geometry. So in the S_1 state this conformational rotation of the phenyl rings is more restricted, which minimizes the non-radiative losses and makes the system highly fluorescent in nature.

C. Mode dependent dynamics from the URLS peak positions

The non-monotonic behaviour observed for the high frequency vibrations gives additional information on the dynamics of excited BPEB. The initial downshift observed for the time dependent peak positions is assumed to be due to electronic delocalization along the conjugation coordinate after photo excitation. The vibrational force constants for the aromatic CC double and CC triple bonds depend on the vibrational coupling among the phenyl and ethynyl units. The strength of the vibrational coupling among the units is determined by the extent of delocalization of electron density over the molecular backbone. We observed ultrafast nuclear relaxation for the CC triple and aromatic CC double bond vibrations. Changes in the electron density influence the electron delocalization and hence cause a reduction in the force constant of the vibrational

frequencies at sub-picosecond time scales.[45–47] The observed rate of the slower frequency upshift also differs for the CC triple and aromatic CC double bonds, as shown in Table III. We have assigned the 8.6 ps and 12.1 ps components as vibrational relaxation (cooling), which could be coupled with torsional degrees of freedom by transferring energy to torsional degrees of freedom and may contribute to the rate of planarization.[48] As discussed above for the URLS intensities, the faster relaxation of the CC triple bonds is probably due to a steeper potential energy surface as compared to the aromatic CC double bonds. In acetonitrile and butyronitrile the frequency upshift is slightly slower as compared to methanol. This has been observed for both bands (CC triple and aromatic CC double bond) and may indicate the above mentioned effect of a hydrophobic solvation shell around the solute in methanol.[44] Interestingly, the rate of relaxation does not change much with solvent viscosity in the same series; very similar rates were observed in acetonitrile (12 ps, 20 ps) and in butyronitrile (12 ps, 19 ps) for the CC triple and CC double bonds, respectively.

V. CONCLUSION

The excited state torsional relaxation and mode-specific dynamics of BPEB in solution phase are reflected in the femtosecond transient absorption (TA) and Ultrafast Raman Loss Spectroscopy (URLS) measurements. Multi-exponential components carry information about ultrafast sub-picosecond structural dynamics, followed by planarization of the partially relaxed, twisted excited state conformers. The flexibility of the molecule is restricted in the excited state because of a much higher rotational barrier, which forces the twisted Franck-Condon species to rotate, and locks the molecule in the most stable planar conformation. This is probably also related to the very high fluorescence quantum yield of BPEB. The time evolution of the excited state Raman band intensities follows structural reorganization. Dynamic polarization of the Raman bands leads to a multi-phase change in intensity. Time dependent downshifts of the peak positions reflect the extent of electron delocalization in the excited electronic state. Sub-picosecond dynamics were observed as URLS frequency shifts, providing short-time dynamical information. In addition, it is evident from the time dependent peak position shifts of the high frequency vibrations that the CC triple bond responds faster to structural changes than the CC double bond. The combination of ultrafast transient absorption and stimulated Raman loss spectroscopy was found to be very powerful for the elucidation of mode-dependent excited state dynamics at picosecond and femtosecond time scales. Further experimental and computational studies are going on in our laboratory to deepen our understanding of BPEB and similar systems, and the results will be published in a forthcoming paper.

SUPPLEMENTARY MATERIAL

See supplementary material for TA kinetic fitting on linear and log scale, transient URLS spectra of BPEB in methanol at shorter and longer time scales, time evolution of the integrated peak areas of the CC double and CC triple bond on linear and logarithmic scale, overlay of fs-TA and URLS kinetics on a logarithmic time scale, and time dependent URLS peak positions of the CC triple bond and CC double bond.

ACKNOWLEDGMENTS

We thank the Council of Scientific and Industrial Research (CSIR), the Department of Science and Technology (DST), and the Defence Research and Development Organization for financial assistance. K.R. and S.K. acknowledge CSIR for a research fellowship. S.U. acknowledges the DST for a J.C. Bose fellowship.

[1] A. S. Blum, J. G. Kushmerick, D. P. Long, C. H. Patterson, J. C. Yang, J. C. Henderson, Y. Yao, J. M. Tour, R. Shashidhar, and B. R. Ratna, Nat. Mater. **4**, 167 (2005); M. S. Khan, A. K. Kakkar, N. J. Long, J. Lewis, P. Raithby, P. Nguyen, T. B. Marder, F. Whittmann, and R. H. Friend, J. Mater. Chem. **4**, 1227 (1994).
[2] C. Joachim, J. K. Gimzewski, and A. Aviram, Nature **408**, 541 (2000).
[3] K. P. Ghiggino, A. J. Tilley, B. Robotham, and J. M. White, Faraday Discuss. **177**, 111 (2015).
[4] R. R. Frontiera and R. A. Mathies, Laser Photonics Rev. **5**, 102 (2011).
[5] I. K. Lednev, T.-Q. Ye, P. Matousek, M. Towrie, P. Foggi, F. V. R. Neuwahl, S. Umapathy, R. E. Hester, and J. N. Moore, Chem. Phys. Lett. **290**, 68 (1998); N. Biswas and S. Umapathy, *ibid.* **236**, 24 (1995).
[6] P. Hamm, S. M. Ohline, and W. Zinth, J. Chem. Phys. **106**, 519 (1997); P. Hamm, M. Zurek, T. Röschinger, H. Patzelt, D. Oesterhelt, and W. Zinth, Chem. Phys. Lett. **268**, 180 (1997).
[7] D. W. McCamant, P. Kukura, and R. A. Mathies, J. Phys. Chem. B **109**, 10449 (2005).
[8] A. Wand, B. Loevsky, N. Friedman, M. Sheves, and S. Ruhman, J. Phys. Chem. B **117**, 4670 (2013).
[9] R. R. Frontiera, J. Dasgupta, and R. A. Mathies, J. Am. Chem. Soc. **131**, 15630 (2009).
[10] A. Wand, R. Rozin, T. Eliash, K. H. Jung, M. Sheves, and S. Ruhman, J. Am. Chem. Soc. **133**, 20922 (2011).
[11] M. C. Smith, J. A. Snyder, B. C. Streifel, and A. E. Bragg, J. Phys. Chem. Lett. **4**, 1895 (2013).
[12] C. Schnedermann, M. Liebel, and P. Kukura, J. Am. Chem. Soc. **137**, 2886 (2015).
[13] T. Takaya and K. Iwata, Analyst **141**, 4283 (2016).
[14] C. Fang, R. R. Frontiera, R. Tran, and R. A. Mathies, Nature **462**, 200 (2009).
[15] C. Schnedermann, V. Muders, D. Ehrenberg, R. Schlesinger, P. Kukura, and J. Heberle, J. Am. Chem. Soc. **138**, 4757 (2016).
[16] J. M. Rhinehart, J. R. Challa, and D. W. McCamant, J. Phys. Chem. B **116**, 10522 (2012).
[17] S. Takeuchi, S. Ruhman, T. Tsuneda, M. Chiba, T. Taketsugu, and T. Tahara, Science **322**, 1073 (2008).
[18] L. Dobryakov, M. Quick, I. N. Ioffe, A. A. Granovsky, N. P. Ernsting, and S. A. Kovalenko, J. Chem. Phys. **140**, 184310 (2014).
[19] J. M. Tour, A. M. Rawlett, M. Kozaki, Y. Yao, R. C. Jagessar, S. M. Dirk, D. W. Price, M. A. Reed, C. Zhou, J. Chen, W. Wang, and I. Campbell, Chem. - Eur. J. **23**, 5118 (2001).
[20] J. Chen, M. A. Reed, A. M. Rawlett, and J. M. Tour, Science **80**, 1550 (1999).
[21] A. Beeby, K. Findlay, P. J. Low, and T. B. Marder, J. Am. Chem. Soc. **124**, 8280 (2002).
[22] J. S. Melinger, Y. Pan, V. D. Kleiman, Z. Peng, B. L. Davis, D. McMorrow, and M. Lu, J. Am. Chem. Soc. **124**, 12002 (2002).
[23] Q. Chu and Y. Pang, Spectrochim. Acta, Part A **60**, 1459 (2004).
[24] A. Beeby, K. S. Findlay, P. J. Low, T. B. Marder, P. Matousek, A. W. Parker, S. R. Rutter, and M. Towrie, Chem. Commun. **2003**, 2406.
[25] S. J. Greaves, E. L. Flynn, E. L. Futcher, E. Wrede, D. P. Lydon, P. J. Low, S. R. Rutter, and A. Beeby, J. Phys. Chem. A **110**, 2114 (2006).
[26] M. Levitus, K. Schmieder, H. Ricks, K. D. Shimizu, U. H. F. Bunz, and M. A. Garcia-Garibay, J. Am. Chem. Soc. **123**, 4259 (2001).
[27] P. V. James, P. K. Sudeep, C. H. Suresh, and K. G. Thomas, J. Phys. Chem. A **110**, 4329 (2006).

[28]M. I. Sluch, A. Godt, U. H. F. Bunz, and M. A. Berg, J. Am. Chem. Soc. **123**, 6447 (2001).
[29]S. Umapathy, A. Lakshmanna, and B. Mallick, J. Raman Spectrosc. **40**, 235 (2009).
[30]R. R. Frontiera and R. A. Mathies, J. Chem. Phys. **127**, 124501 (2007).
[31]S. Umapathy, K. Roy, S. Kayal, N. K. Rai, and V. Ravikumar, "Structure and dynamics from time resolved absorption and Raman spectroscopy," *The Future of Dynamic Structural Science*, edited by J. A. K. Howard, H. A. Sparkes, P. R. Raithby, and A. V. Churakov (Springer, 2014), pp. 25–42.
[32]R. R. Frontiera, S. Shim, and R. A. Mathies, J. Chem. Phys. **129**, 064507 (2008); S. Umapathy, B. Mallick, and A. Lakshmanna, *ibid.* **133**, 024505 (2010).
[33]B. Mallick, A. Lakhsmanna, and S. Umapathy, J. Raman Spectrosc. **42**, 1883 (2011).
[34]R. R. Frontiera, C. Fang, J. Dasguptac, and R. A. Mathies, Phys. Chem. Chem. Phys. **14**, 405 (2012).
[35]A. Lakhsmanna, B. Mallick, and S. Umapathy, Curr. Sci. **97**, 210 (2009).
[36]P. Kukura, D. W. McCamant, and R. A. Mathies, Annu. Rev. Phys. Chem. **58**, 461 (2007).
[37]U. Harbola, S. Umapathy, and S. Mukamel, Phys. Rev. A **88**, 011801 (2013).
[38]N. K. Rai, A. Y. Lakshmanna, V. V. Namboodiri, and S. Umapathy, J. Chem. Sci. **124**, 177 (2012).
[39]F. Ariese, K. Roy, V. Ravi Kumar, H. C. Sudeeksha, S. Kayal, and S. Umapathy, *Encyclopedia of Analytical Chemistry* (John Wiley and Sons, 2016).
[40]D. R. Klug, T. Rech, D. M. Joseph, J. Barber, J. R. Durrant, and G. Porter, Chem. Phys. **194**, 433 (1995).
[41]D. M. Jonas, M. J. Lang, Y. Nagasawa, T. Joo, and G. R. Fleming, J. Phys. Chem. **100**, 12660 (1996).
[42]J. Hofkens, L. Latterini, G. D. Belder, T. Gensch, M. Maus, T. Vosch, Y. Karni, G. Schweitzer, F. C. D. Schryver, A. Hermann, and K. Mullen, Chem. Phys. Lett. **304**, 1 (1999).
[43]S. Wallin, J. Davidsson, J. Modin, and L. Hammarstro, J. Phys. Chem. A **109**, 4697 (2005).
[44]V. Ravi Kumar, C. Verma, and S. Umapathy, J. Chem. Phys. **144**, 064302 (2016).
[45]W. Yu, P. J. D. Vallett, J. Zhou, and A. E. Bragg, J. Chem. Phys. **141**, 044201 (2014).
[46]C. Castiglioni, M. D. Zoppo, and G. Zerbi, J. Raman Spectrosc. **24**, 485 (1993).
[47]G. Zerbi, C. Castiglioni, and M. D. Zoppo, *Electronic Materials: The Oligomer Approach* (Wiley, 2008).
[48]J. Briand, O. Bräm, J. Réhault, J. Léonard, A. Cannizzo, M. Chergui, V. Zanirato, M. Olivucci, J. Helbing, and S. Haacke, Phys. Chem. Chem. Phys. **12**, 3178 (2010).